Improved chopping of a lithium beam for plasma edge diagnostic at ASDEX Upgrade

M. Willensdorfer,[1, a)] E. Wolfrum,[2, b)] R. Fischer,[2] J. Schweinzer,[2] M. Sertoli,[2] B. Sieglin,[2] G. Veres,[3] F. Aumayr,[1] and the ASDEX Upgrade Team

[1)] *Institute of Applied Physics, Vienna University of Technology, Association EURATOM-ÖAW, A-1040 Vienna, Austria*

[2)] *Max-Planck-Institut für Plasmaphysik, Association EURATOM, D-85748 Garching, Germany*

[3)] *KFKI-RMKI, Association EURATOM, Pf. 49, H-1525 Budapest, Hungary*

The lithium beam diagnostic at ASDEX Upgrade routinely delivers electron density profiles in the plasma edge by lithium beam impact excitation spectroscopy. An accurate background subtraction requires a periodically chopped lithium beam. A new, improved chopping system was developed and installed. It involves a voltage modulation for the extractor electrode and the beam deflection plates. The modulation of the extractor electrode reduces the unused portion of lithium ions and improves the stability of the beam with respect to its position. Furthermore, the data indicate an extended emitter lifetime. The extractor chopping was also found to be insensitive to sparks. The deflection chopping experiments demonstrated beam chopping in the kHz range. The significantly higher modulation frequency of the deflection chopping improves background subtraction of fast transient events. It allows a more accurate density measurements in the far scrape off layer during impurity injections and edge localized modes.

Keywords: Lithium beam, tokamak, ASDEX Upgrade, plasma diagnostics

[a)] Electronic mail: willensdorfer@iap.tuwien.ac.at

[b)] Electronic mail: elisabeth.wolfrum@ipp.mpg.de

I. INTRODUCTION

The high confinement mode (H-mode) is the foreseen scenario for ITER. The confinement and the general performance of ITER strongly depend on the plasma edge properties. It is essential to be able to measure and characterize plasma edge parameters with a high temporal and spatial resolution.

The lithium beam diagnostic at ASDEX Upgrade has been routinely used to measure electron density profiles in the plasma edge by lithium beam impact excitation spectroscopy (Li-IXS)[1]. Nowadays, lithium beam diagnostics are in operation at several fusion devices, e.g. COMPASS[2], DIII-D[3], JET[4] and TEXTOR[5]. The method is based on excitation from collisions of injected lithium atoms and plasma particles[6]. The beam light emission depends highly on the plasma electron density. Numerical techniques were developed to evaluate the electron density from the light intensity[1,7,8]. To subtract the background accurately, a chopping of the lithium beam is necessary. So far, we used deflection plates to modulate the beam. This system was not optimized for high chopping frequencies. As a result, the background evolution of fast events, e.g., during edge localized modes (ELMs), could not be treated appropriately. We renewed and optimized the deflection chopping system. We also built a second chopping system to realize the beam modulation via extraction voltage

This paper is arranged into 4 sections. Section II describes the setup of the lithium beam diagnostic and both new chopping systems. Section III compares both systems and illustrates the advantages and disadvantages of each system, but with focus on the extraction chopping technique. Section IV deals with the effect of fast events, e.g. ELMs or Ar injections, on electron density profile reconstruction with and without proper treatment of the background signals.

II. CHOPPING SYSTEM OF THE LITHIUM BEAM DIAGNOSTIC

The designs of lithium beam diagnostics have often been described[9,10]. Therefore, we will only give a brief description of the experimental setup at ASDEX Upgrade. Fig. 1 shows a sketch of the diagnostic setup. The lithium ions are extracted from an β-eucryptite emitter, then focused and accelerated to up to 60 keV. Before they enter a sodium (Na) neutralizer cell, the ions pass two deflection plates. The neutral lithium atoms are injected from the low

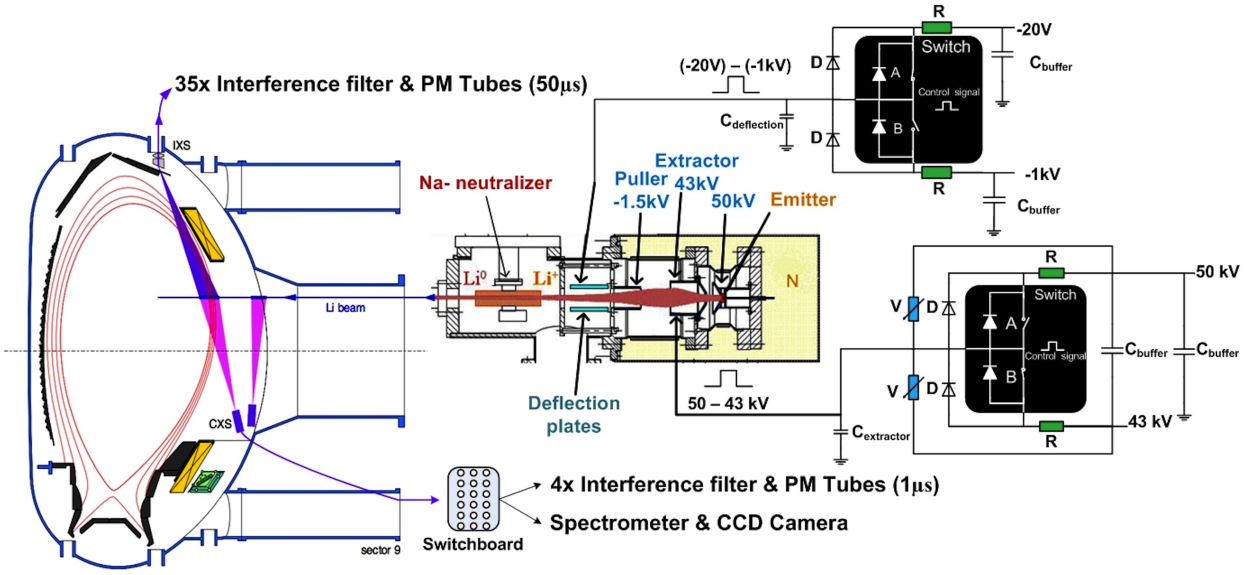

FIG. 1. This sketch shows the experimental setup of the lithium beam diagnostic at ASDEX Upgrade. The electrical circuits of the deflection and extraction modulation system are illustrated.

field side (LFS). Two optical heads are installed, which are focused along the beam line. The so called Li-IXS optics measure Li (2p-2s) line emission from above using photomultiplier tubes (PMTs) and interference filters. This system has a time resolution of 50 μs. A second optical head, below the lithium beam, is mainly used to observe beam-plasma interaction by lithium beam activated charge exchange spectroscopy (Li-CXS)[11,12]. We have two Cerny-Turner spectrometers with charge coupled device (CCD) cameras and a temporal resolution of 4 ms. Additional 4 interference filters and PMTs with a time resolution of 1 μs are connected to the switchboard of the lower Li-CXS optics[13].

In principle, we have two possibilities to chop the lithium beam. First, we can vary the voltage of one deflection plate to hop the beam aside the optics. Second, we can modulate the extraction voltage to suppress the extraction periodically. The first method was routinely used before and is commonly used in lithium beam diagnostics at other fusion devices. We modified our deflection chopping system by using a push pull circuit[14]. The key component of our setup is a high voltage (HV) MOSFET switch from Behlke[15] (HTS-31-03-GSM), which can modulate up to 3 kV with a frequency of 40 kHz. To reduce the cable length we mounted the setup directly above the lithium injector. This position requires an iron shielding due to an internal DC-to-DC converter, which does not work in the stray magnetic field of the tokamak. We installed resistors (49 & 22 Ω) and damping diodes (BY 558)

to avoid damage on the switch. Buffer capacitors (1 μF) deliver the necessary currents to charge and discharge the intrinsic capacity of the cables and deflection plate within less than a microsecond.

The second chopping system, which modulates the extraction voltage, was used for the first time for a lithium beam diagnostic. In order to realize chopping via extraction we modulate the extractor electrode voltage between the conventional extraction value (43 kV) and the acceleration value (50 kV), Fig. 1. The principles of the electrical circuit are the same as before. We installed a MOSFET switch from Behlke (HTS-161-06-GSM), which is able to switch up to 16 kV. A galvanic isolation of 80 kV between the control and the HV devices was also implemented. We switch up to 8 kV at a voltage level of $30 - 60$ kV, which is well within the capabilities of the HV switch. This setup requires the use of HV resistors (1 kΩ), damping diodes (SCHJ 15K) and buffer capacitors (50 nF). Varistors are added to avoid a breakdown of the switch during sparks. For safety reasons, we mounted the circuit behind the injector in a grounded cage with a volume of 1 m^3. Again, an iron shielding was necessary, preventing the switch from malfunctioning during plasma discharges because of the stray magnetic field.

III. PERFORMANCE OF THE NEW SYSTEMS

A. Rising edges

The performance of the chopping systems depends strongly on the rising and falling edges. Therefore, we chose the lowest possible values for the resistors, but still high enough to limit the currents to avoid damage. The switch for extraction chopping allows a maximum peak current of 60 A, which gives us a resistance value of at least 1 kΩ for a maximum emitter voltage of 60 kV. Assuming an intrinsic capacity of 700 pF, the time constant $\tau = RC$ amounts to 0.7 μs. In the case of the deflection chopping system, we achieve even shorter rising and falling edges. The low modulation voltage allows resistor values of 49 and 22 Ω. We assume a capacity of 400 pF, which gives us a time constant of 20 ns. Fig. 2 compares the rising edges of the two new systems and the old system during plasma discharges with a long, constant density phase. The data were sampled with a temporal resolution of 1 μs to evaluate the time evolution of rising edges. Because of the limited resolution we plot several

edges in one panel. We use a least square fit of an exponential function to determine the time constant of the three different systems. Fig. 2(a) and (b) show rising edges from the new enhanced systems and Fig. 2(c) shows measurements from the old chopping system. Please note that the x-axis scaling of Fig. 2(c) differs from the other ones by a factor of 100. We improved the transition speed by about 3 orders of magnitude. Because of these short transition times, we are now able to consider more data points for n_e evaluation during the beam on phase.

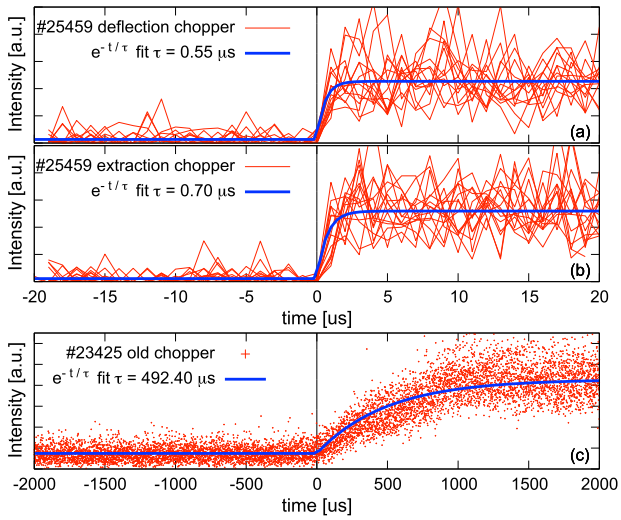

FIG. 2. Emission time traces relative to the onset of the rising edges for deflection (a), extraction (b) and the old (c) chopping system.

B. Chopping via extraction

Chopping the beam by modulating the extraction voltage is highly advantageous. The portion of unused lithium atoms reduces, which extends the emitter lifetime. The data from the new setup suggest that the amount of sparks is reduced, but this conclusion is difficult to quantify, as many factors might play a role, such as voltages and gas pressure.

From earlier measurements we observed a higher light emission intensity during the build up phase of the lithium beam. It was assumed that the voltage turn-on causes this intensity gain. Additionally, we hoped that the emitter would benefit from the relaxation or a diffusion process during the *beam off* phase and that it might also result in an increased intensity. This increase in intensity was not observed. A comparison of the ion current with and without

extraction chopping can be seen in Fig. 3(a). It shows current measurements using a faraday cup at the end of the injector beam line. The time range, when we modulated the extraction voltage and when not, are labelled. As seen in Fig. 3(a), the hoped increased intensity was not observed during this experiment and during plasma discharge experiments. Instead, we observe a more stable beam with respect to its position during chopping by extraction. In Fig. 3(a) we can clearly identify that the measured current fluctuates much less, when we use extraction modulation. These measurements also show an instability of the beam at around 15 seconds where the ion beam destabilizes and the measured current drops. We assume that charging up of unidentified components deflects the beam, which results in a drop in the faraday cup measurement. Chopping of the extractor reduces such charging. Hence, the beam is more stable with respect to its position

The ion consumption can be measured by the current supply, since they are directly proportional to each other. A comparison of the supply current with and without extractor chopping during a plasma discharge, is given in Fig. 3(b). The modulation of the extractor electrode leads to a modulation of the current supply. These measurements were done with a relatively old emitter, hence the strongly decreasing current. If we compare the current decay, we see that the decay is lower with extractor modulation. Which means, with extraction modulation the lithium current remains higher at the end of the discharge.

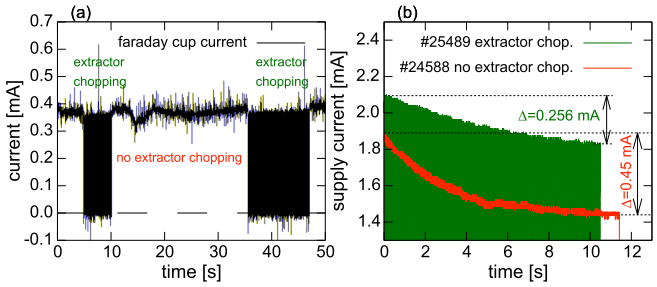

FIG. 3. The left figure shows faraday cup measurements of the lithium ion beam. The right figure shows the current of the power supply during two subsequent plasma discharges.

The switch was operating during the ASDEX Upgrade campaigns 2009 and 2011. Because of the carefully designed protection system the switch was not damaged and survived about several hundred sparks.

The maximum frequency of the system is limited by an upper switching frequency of 2 kHz, a maximum current of the power supply and a maximum power dissipation of the

switch (20 W). The current of the switching process and the power dissipation are given by

$$I = C_{int}\, U_w\, f \tag{1}$$

and

$$P_{diss} = \frac{C_{int}\, U_w^2\, f}{2} \tag{2}$$

where U_w is the working voltage, f the frequency and C_{int} the intrinsic capacity. Assuming, U_w is 7 kV and C_{int} is 700 pF, we get a maximum frequency of 1.17 kHz for a power dissipation of 20 W. Because of the limits of the power supply current, we could only achieve 250 Hz. For fast transient events like ELMs a modulation frequency of about 250 Hz would not be sufficiently high to allow an accurate background subtraction. Therefore, we also need a modulation by deflection to study the background evolution during ELMs and its effect on electron density profiles.

C. Comparison to chopping via deflection

The big advantage of the beam deflection technique is that we can easily reach high frequencies[14]. Because of low voltages the frequency is only limited by the hardware specifications. The small size of the setup is an additional advantage. On the other hand, almost all benefits from the extraction modulation, i.e., more stable position, extended emitter lifetime, etc, are missing. Table I shows a qualitative comparison of both systems.

IV. EXPERIMENTAL RESULTS IN ASDEX UPGRADE

A. Experimental spectra

Sources of background emission are Bremsstrahlung and characteristic line emission. Bremsstrahlung depends on the electron density, electron temperature and the amount of impurities. More difficult is the consideration of the characteristic line emission and its contribution to the background emission. Fig. 4(a) shows a typical spectrum measured by the Li-CXS system during a plasma discharge. The wavelength of Li I ($2p - 2s$) transition amounts to 670.8 nm. Because of the lithium injection velocity and the different viewing angles of the two optical systems, we measure a blue Doppler shifted Li I line by the Li-IXS

TABLE I. Tabular overview of the given and calculated values of both circuits.

Technique:	Extraction	Deflection
intrinsic capacity (C_{int}):	~ 700 pF	~ 400 pF
breakdown voltage:	18 kV	4 kV
max. current of switch (I_{max}):	60 A	30 A
max. used frequency (f):	250 Hz	2 kHz
power dissipation (P_{max}):	20 W	10 W
used resistors:	1 $k\Omega$	49 & 22 Ω
used working voltage (U_w):	7 kV	1 kV
calculated $\tau = R\,C_{int}$:	> 400 ns	> 9.8 ns
measured τ:	< 700 ns	< 550 ns
max. possible frequency f:	1.16 kHz	40 kHz

optics and a red shifted line by the Li-CXS optics. Fig. 4(a) illustrates the position of the blue Doppler shifted and the unshifted Li I line by vertical lines. It also shows the wavelength dependency of the transmission coefficient of one interference filter. The installed interference filters cover part of a helium line (He I), which is rather pronounced directly after a He glow discharge. Beside the He I line the filters also cover lines of nitrogen (N I, Fig. 4b), argon (Ar II, Fig. 4(c)) and tungsten (W I). We observe a clear increase of the background signal, when one of these impurities is injected via gas puffing or laser blow off.

B. Argon gas injection

As mentioned in the last section, the injected Ar gas rises the background signal, which is mainly due to the Ar II line emission at 668.4 nm (Fig. 4(c)). Before the ASDEX Upgrade campaign in 2009, we used modulation periods of 56 ms for *beam on* and 24 ms for *beam off*[1]. In the case of Ar puffing or seeding this is far too slow. Therefore, we reduced the *beam on* and *beam off* periods to 8 ms and 4 ms, respectively, to be able to subtract the background signal appropriately. The argon injection is visible in Fig. 5 from the evolution of the core argon concentration, evaluated using a Johann crystal spectrometer which is optimized for the measurement of He-like (16+) argon resonance lines[16]. Fig. 5 also shows

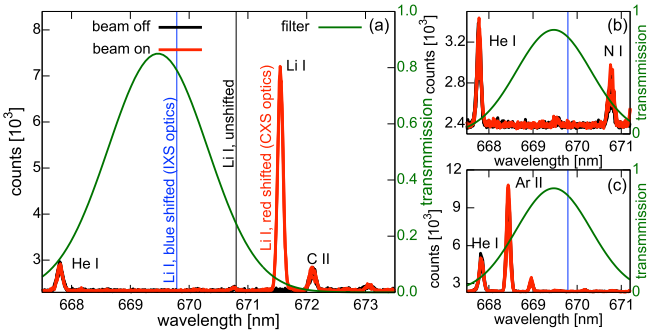

FIG. 4. (a) spectrum of an usual plasma discharge observed with one channel of the Li-CXS optics (lower optics) in the wavelength range of the *Li I* line (unshifted, black). The Li-CXS optics observes a red shifted line and Li-IXS optics a blue shifted line indicated by a vertical blue line. The transmission coefficient $T(\lambda)$ of one interference filters of the Li-IXS optics (upper optics) is also shown. Panels (b) and (c) show the same spectrum during nitrogen seeding and argon puffing.

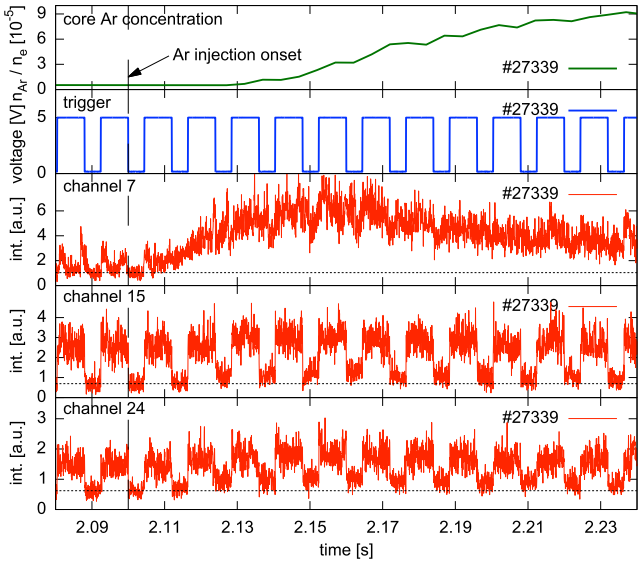

FIG. 5. Time traces (top to bottom): Core Ar concentration, trigger signal of the beam modulation (TTL high $\hat{=}$ *beam on*) and raw signals of 3 channels of the Li-IXS optics during an Ar injection. The horizontally dotted lines indicate the mean of the background signals prior to the Ar injection.

the trigger signal for the Li beam modulation and raw signals of three channels (7, 15 and 24), where 7 is situated in the limiter shadow, 15 in the scrape off layer (SOL) and 24 within the separatrix. All channels show a sudden rise of the signal, which originates from radiation of the injected Ar gas. The time delay between the Li-IXS and the Johann crystal

spectrometer measurements is due to the different measured ionization stages and thus to the different radial position of emissivity, the first in the limiter shadow and SOL, the second around mid radius. This delay is in line with typical argon transport observed at ASDEX Upgrade[16].

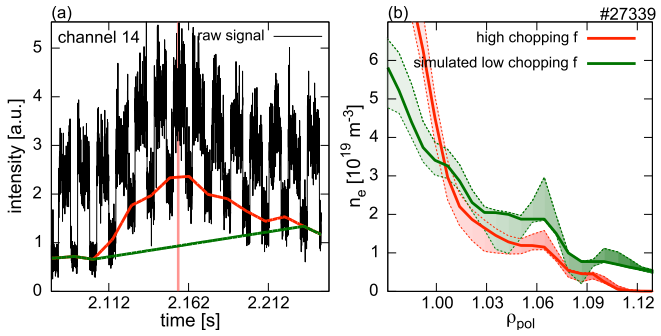

FIG. 6. (a) time trace of channel 14 of the Li-IXS optics. The colored lines indicate the different cases for background subtraction. The vertical bar shows the evaluated time window (1 ms). (b) evaluated n_e profiles for the different cases of (a). The shaded areas indicate the uncertainties.

To study the effect of an inaccurate background subtraction on the n_e profile reconstruction, we evaluated n_e profiles for two different cases. We calculated all n_e profiles using the probabilistic lithium beam data analysis[1]. The first case is the default case, in which we calculate the median of every *beam off* phase and then we interpolate linearly in between (Fig. 6a, red curve). For the second case we calculate the median of the *beam off* phases prior and after the Ar injection onset and then we interpolate in between to simulate a low chopping frequency (Fig. 6(a), green curve). This second case is comparable to the conventional chopping times of 56 ms vs 24 ms. Fig. 6(b) shows the reconstructed n_e profiles over normalized poloidal flux surfaces (ρ_{pol}) of these two cases. We observe that the n_e evaluation clearly overestimates the n_e in the SOL when we use an inaccurate background subtraction (Fig. 6(b), green curve). Furthermore, the n_e profile is more flat than in reality. Note, this overestimation depends strongly on the amount of the injected gas. This example shows that we can significantly increase the measurement accuracy by increasing the chopping frequency. The same situation is given, when we inject other impurities, e.g., tungsten via laser blow off or nitrogen via gas injection. For all these impurity injections a sufficient fast beam modulation is essential.

C. Edge localized modes (ELMs)

In the case of ELMs the situation is even more challenging than for impurity injections. ELMs occur on a millisecond timescale, which means that we need a beam modulation at least in the kHz range. We can only achieve such high frequencies by chopping via deflection. We chose a frequency of 2 kHz, which is fast enough for ELMs and slow enough to obtain sufficient data points during *beam on* phases. Fig. 7 shows the evolution of the background signal during one ELM. We subtracted the mean of the ELM free phase from the signal. The background signal suddenly increases after the ELM crash (mainly in outermost channels, $\#1 - 10$).

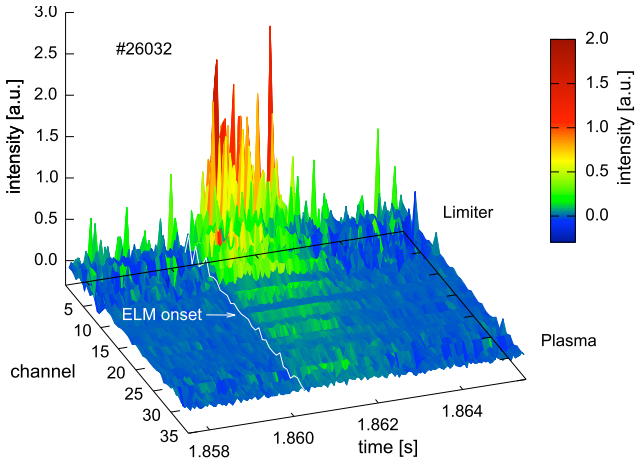

FIG. 7. The mean of the ELM free phase is subtracted from the calibrated background signal of all Li-IXS optics channel during one ELM. ELMs strongly increase the background signal of the outermost channels of the Li-IXS optics.

The rise of the background radiation originates from an increased line radiation because of impact excitation induced by the sudden particle exhaust and an increased Bremsstrahlung. This radiation depends strongly on the impurity content. To compare n_e profiles using kHz modulation with n_e profiles using conventional chopping, we changed the modulation frequency between two almost identical H-mode discharges (#27088 and #27089). These two discharges were performed after a short opening, where the impurity content is usually high and the background increased during an ELM. Fig. 8 shows time traces of both discharges. During #27088 we applied the 20 Hz modulation (red) and during #27089 the

2 kHz chopping (blue), which is evident from the trigger signal and the Li-IXS channels in Fig. 8. We use the divertor current to identify ELM events.

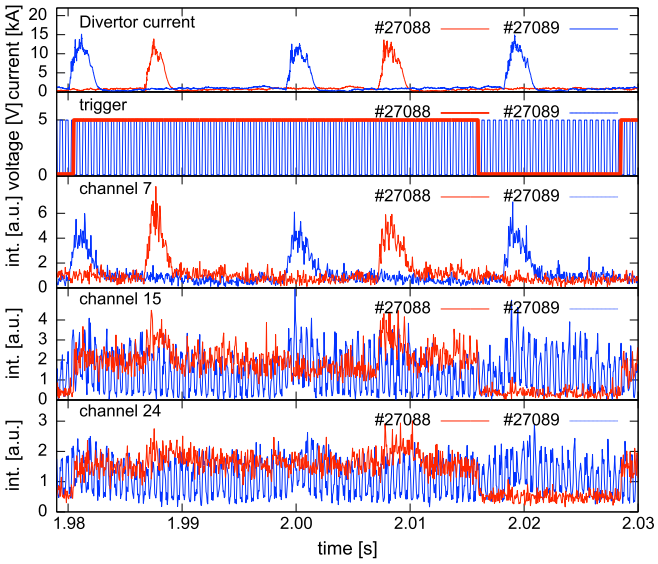

FIG. 8. Time traces (top to bottom): divertor current, trigger signal of the beam modulation (TTL high $\hat{=}$ *beam on*) and raw signal of 3 channels of the Li-IXS optics during two subsequent discharges (red, #27088 and blue, #27089).

To detect any difference in the observed electron density, we pick two ELMs, one of each discharge, where heating and line density were similar. Then, we evaluate n_e profiles prior and during the ELM. Fig. 9(a) and (b) show calculated n_e profiles, when using 2 kHz and 20 Hz modulation, respectively. We observe almost identical inter ELM profiles, which was expected. However, the n_e profiles at the maximum particle exhaust during the ELM show significant differences. First, the 2 kHz chopping profile (Fig. 9(b)) reveals that we have almost no electron density for $\rho_{pol} > 1.09$. This is not observed when we chop slower. Second, we observe an n_e kink between ρ_{pol} of 1.07 and 1.09, where the n_e sharply decreases. Third, the n_e profiles from $\rho_{pol} = 1$ to 1.04 seem to remain steeper during the ELM. These profile features are visible in almost all observed ELMs during this H-mode.

To verify the conclusions from the previous comparison, we take data from the 2 kHz modulation and simulate the conventional background subtraction. We calculate the median of the chopped beam before and after the ELM when the plasma edge is unperturbed. Then, we interpolate in between and use this as input for the n_e reconstruction. Fig. 10(a) shows the two simulated backgrounds and the corresponding raw signal of channel 11. The evaluated

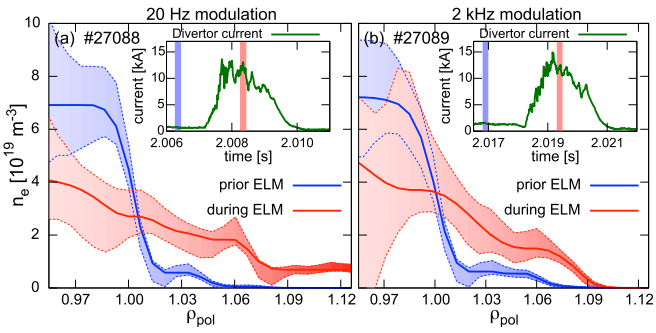

FIG. 9. (a) n_e profiles before and during an ELM using 20 Hz chopping. (b) n_e profiles before and during an ELM using 2 kHz chopping. The shaded areas indicate the uncertainties. The inserts show the corresponding divertor current and the vertical bars indicate the evaluated time windows (160 μs).

n_e profiles verify the previous results (Fig. 10(b)). Again, we observe an overestimated n_e in the SOL and a flatter profile when using conventional background subtraction.

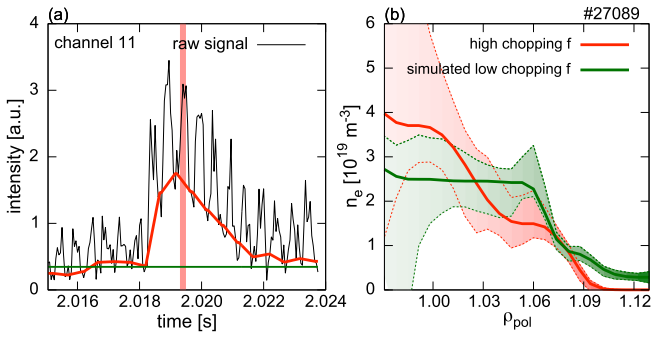

FIG. 10. (a) time trace of channel 16 of the Li-IXS optics. The colored lines indicate the different cases for background subtraction. The vertical bar indicates the evaluated time window (160μs). (b) evaluated n_e profiles for the two cases of (a). The shaded areas indicate the uncertainties.

The steepening of the n_e profile between ρ_{pol} of 1.07 and 1.09 during the ELM (Fig. 10) originates from the limiter position relative to the plasma shape. Fig. 11 illustrates the position of Li-IXS channels, the limiter contours and flux surfaces from equilibrium reconstruction. The n_e values of the corresponding channels are shown in the small insert. The limiter structure clearly limits the n_e, even in the presence of a sudden particle exhaust caused by an ELM.

Note, during these experiments the impurity content was relatively high and the impact

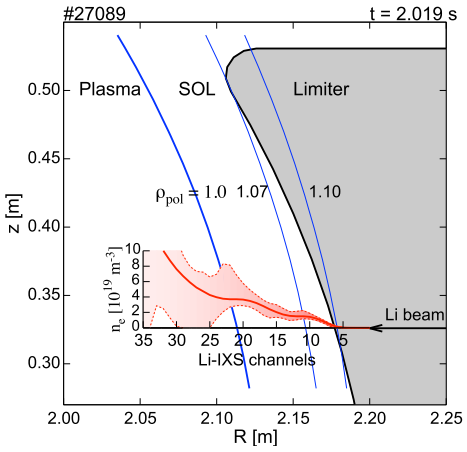

FIG. 11. Position of the limiter (grey) and the measured n_e profile (red) over the channel position of Li beam during an ELM at the maximum particle exhaust. The blue lines show the position of the normalized flux surfaces. The n_e is clearly limited by the limiter, even in the presence of an ELM. The shaded area indicates the uncertainties

of the ELMs on the background signal very pronounced. Therefore, our conclusions about the n_e in the SOL and the profile steepness are specifically for these particular conditions. For a lower impurity content the effect of proper background subtraction is less strong.

V. CONCLUSIONS

We successfully installed and applied the extraction chopping technique on the ASDEX Upgrade lithium beam diagnostic. We observe a longer emitter lifetime, a more stable beam with respect to its position and less sparks. Our setup is also surprisingly insensitive to sparks because of a carefully designed protection system. In principle, the rising edges and the maximum power dissipation of the switch would allow a modulation frequency of 1 kHz, but our power supply limits the frequency to 250 Hz. We optimized our deflection technique with a new, fast, small and robust system. The new chopping systems allow us to resolve fast transient plasma events with appropriate background subtraction.

We analyzed the impact of the improved background subtraction on the n_e reconstruction. We showed overestimated electron densities n_e in the SOL and underestimated n_e gradients around the separatrix during fast transient events, e.g. ELMs, when beam chopping is too slow.

Due to its key benefits, we use the modulation via extraction routinely. We switch to chopping via deflection, when accurate electron density profiles during ELMs are needed. Especially under conditions of a high impurity content, an accurate background estimation during ELMs becomes crucial.

ACKNOWLEDGMENTS

M. Willensdorfer is a fellow of the Friedrich Schiedel Foundation for Energy Technology. The author would like to thank M. Ebner, H. Eixenberger, K. Klaster and their groups for hospitality and constructive discussions. This work, supported by the European Commission under the Contract of Association between EURATOM and ÖAW, was carried out within the framework of the European Fusion Development Agreement (EFDA). The views and opinions expressed herein do not necessarily reflect those of the European Commission.

REFERENCES

[1]R. Fischer, E. Wolfrum, J. Schweinzer, and the ASDEX Upgrade Team, Plasma Physics and Controlled Fusion **50**, 085009 (2008).

[2]I. Pusztai, G. Pokol, D. Dunai, D. Refy, G. Por, G. Anda, S. Zoletnik, and J. Schweinzer, Review of Scientific Instruments **80**, 083502–083508 (2009).

[3]D. Thomas, Review of Scientific Instruments **74**, 1541–1546 (2003).

[4]M. Brix, D. Dodt, A. Korotkov, P. Morgan, D. Dunai, R. Fischer, A. Meigs, I. Nedzelskiy, J. Schweinzer, J. Vince, S. Zoletnik, and JET-EFDA Contributers, Review of Scientific Instruments **81**, 10D733–4 (2010).

[5]D. Dunai, S. Zoletnik, G. Anda, G. Petravich, S. Kalvin, J. Sarkozi, A. Kramer-Flecken, B. Schweer, and the TEXTOR team, 36th EPS Conference on Plasma Phys. **33E**, 1–4 (2009).

[6]J. Schweinzer, R. Brandenburg, I. Bray, R. Hoekstra, F. Aumayr, R. K. Janev, and H. P. Winter, Atomic Data and Nuclear Data Tables **72**, 239–273 (1999).

[7]J. Schweinzer, E. Wolfrum, F. Aumayr, and M. Pöckl, Plasma Physics and Controlled Fusion **34**, 1173–1183 (1992).

[8]R. Brandenburg, J. Schweinzer, S. Fiedler, and F. Aumayr, Plasma Physics and Controlled Fusion **41**, 471–484 (1999).

[9]K. McCormick, S. Fiedler, G. Kocsis, J. Schweinzer, and S. Zoletnik, Fusion Engineering and Design **34-35**, 125–134 (1997).

[10]E. Wolfrum, F. Aumayr, D. Wutte, H. Winter, E. Hintz, D. Rusbuldt, and R. Schorn, Review of Scientific Instruments **64**, 2285–2292 (1993).

[11]R. Schorn, E. Hintz, D. Rusbüldt, and F. Aumayr, Applied Physics B: Lasers and Optics **52**, 71–78 (1991).

[12]E. Wolfrum, J. Schweinzer, M. Reich, L. Horton, and the ASDEX Upgrade Team, Review of Scientific Instruments **77**, 033507 (2006).

[13]D. Dunai, S. Zoletnik, J. Sarkozi, and A. Field, Review of Scientific Instruments **81**, 103503–8 (2010).

[14]S. Zoletnik, G. Petravich, A. Bencze, M. Berta, S. Fiedler, K. McCormick, J. Schweinzer, and the W7-AS Team, Review of Scientific Instruments **76**, 073504–12 (2005).

[15]F. Behlke, "General instructions and datasheets from Behlke Power Electronics GmbH, http://www.behlke.de,".

[16]M. Sertoli, C. Angioni, R. Dux, R. Neu, T. Pütterich, V. Igochine, and the ASDEX Upgrade Team, Plasma Physics and Controlled Fusion **53**, 035024 (2011).